Proceedings of FEDSM2008
2008 ASME Fluids Engineering Conference
August 10-14, 2008 Jacksonville, Florida USA

FEDSM2008-55143

EULER-EULER LARGE-EDDY SIMULATION APPROACH FOR NON ISOTHERMAL PARTICLE-LADEN TURBULENT JET

Enrica Masi
Institut de Mécanique des Fluides de Toulouse
UMR 5502 CNRS / INPT / UPS
Allée du Professeur Camille Soula,
31400 Toulouse, France
masi@imft.fr

Benoît Bédat
Institut de Mécanique des Fluides de Toulouse
UMR 5502 CNRS / INPT / UPS
Allée du Professeur Camille Soula
31400 Toulouse, France
bedat@imft.fr

Mathieu Moreau
Lab. Transferts Écoulements Fluides Énergétique
UMR8508 CNRS/ENSAM/ENSCPB/U.Bordeaux1
16, avenue Pey-Berland
33607 Pessac Cedex, France
moreau@lmm.jussieu.fr

Olivier Simonin
Institut de Mécanique des Fluides de Toulouse
UMR 5502 CNRS / INPT / UPS
Allée du Professeur Camille Soula
31400 Toulouse, France
simonin@imft.fr

ABSTRACT

This paper presents an Euler-Euler Large-Eddy Simulation (LES) approach for the numerical modeling of non isothermal dispersed turbulent two-phase flows. The proposed approach is presented and validated by *a priori* tests from an Euler-Lagrange database, provided using discrete particle simulation (DPS) of the particle phase coupled with direct numerical simulation (DNS) of the turbulent carrier flow, in a non isothermal particle-laden temporal jet configuration. A statistical approach, the Mesoscopic Eulerian Formalism (MEF) [Février *et al.*, J. Fluid Mech., 2005, vol. 533, pp. 1-46], is used to write local and instantaneous Eulerian equations for the dispersed phase and then, by spatial averaging, to derive the LES equations governing the filtered variables. In this work, the MEF approach is extended to scalar variables transported by the particles in order to develop LES for reactive turbulent dispersed two-phase flows with mass and heat turbulent transport. This approach leads to separate the instantaneous particle temperature distribution in a Mesoscopic Eulerian field, shared by all the particles, and a Random Uncorrelated distribution which may be characterized in terms of Eulerian fields of particle moments such as the uncorrelated temperature variance. In this paper, the DPS-DNS numerical database is presented, LES Eulerian equations for the dispersed phase are derived in the frame of the Mesoscopic approach and models for the unresolved subgrid and random uncorrelated terms are proposed and *a priori* tested using the DPS-DNS database.

Keywords: Euler-Euler LES, two-phase flows, mesoscopic approach, non isothermal planar jet.

INTRODUCTION

Large-Eddy Simulations (LES) for single-phase flows are used in several industrial applications where complex geometries or/and unsteady phenomena occur such as acoustic instabilities in combustion chambers. When a second phase must be taken into account, for example injection of liquid fuel, it is necessary to develop models for the dispersed phase. This is commonly referred to as two-phase flow LES and it represents a promising tool for the future, receiving great attention from scientific and industrial communities. The dispersed phase can be treated in a Lagrangian or Eulerian framework leading to two type of two-phase flow LES approaches: Euler-Lagrange and Euler-Euler LES. In the last decade the Euler-Lagrange approach have been used and several aspects have been investigated [2,3,4,5]. As alternative, the Euler-Euler LES approach (or two-fluid LES) remains still limited because of the great complexity to derive dispersed phase LES equations and models in the Eulerian framework. LES of the Eulerian dispersed phase computes dynamics of

Copyright © 2008 by ASME

Downloaded From: https://proceedings.asmedigitalcollection.asme.org on 06/30/2019 Terms of Use: http://www.asme.org/about-asme/terms-of-use

larger-scale motions while the influence of the smaller scales is modeled since they should have, theoretically, universal character. The choice of approach to obtain the Eulerian particle LES equations plays an important role on the modeling. In the case of inertial particles with relaxation times larger than the Kolmogorov time scale, Fevrier *et al.* [1] shown that a decomposition in correlated and uncorrelated motion (by the Mesoscopic Eulerian Formalism, MEF) can be used to give a better interpretation of velocity distribution. Especially in the frame of spatial filtering application, where Moreau *et al*. [6,24] pointed out different scaling for correlated versus uncorrelated quantities, highlighting the different natures of the two contributions: the MEF approach, by accounting separately for the contributions, allows simplifying sub-grid terms modeling in filtered Mesoscopic equations. Despite that, modeling remains always quite complex considering that the dispersed phase can be compared to a highly compressible fluid with a Mach number largely greater than one [7] for which theory of smaller scales mechanism is still a topical research. In this paper we propose and test classical "low Mach" subgrid fluid model extended to dispersed phase. We also propose and test closure models for the uncorrelated moments issued from statistical continuum approach. Special attention is given to modeling terms issued from the mesoscopic decomposition of the temperature, which needs to be taken into account in order to develop LES for reactive turbulent dispersed two-phase flows. Validation is performed by *a priori* testing using a database obtained from a Discrete Particle Simulation (DPS) for the particles coupled with a Direct Numerical Simulation (DNS) for the carrier flow.

NOMENCLATURE

g_p	particle variable
g_f	fluid variable
$g_{f@p}$	fluid variable « viewed » by the particle
$\breve{g}_p$	mesoscopic particle variable
$\delta\breve{g}_p$	random uncorrelated particle variable
$\hat{g}$	spatial filtered variable

STATISTICAL APPROACH

In the framework of Mesoscopic Eulerian Formalism (see the Appendix for further details) the correlated (Mesoscopic) and uncorrelated (Quasi-Brownian, QB) Eulerian quantities are defined through the moments associated to conditioned probability density function (p.d.f.) $\breve{f}_p^{(1)}$. The transport equations for velocity-temperature function $\psi_p(\boldsymbol{C}_p,\xi_p)$, are obtained by analogy with kinetic theory of dilute gases or dry granular media. In very dilute regime, the inter-particles collisions are assumed negligible as well as the turbulence modulation in the carrier flow equations. Without gravity, for particles with diameter smaller or equal than Kolmogorov length scale and with density much larger than the fluid one, only drag force modify the pdf. If the inter-phase heat transfers are considered stationeries, the p.d.f. equation is closed as follows:

$$\frac{\partial}{\partial\tau}\breve{f}_p^{(1)}+\frac{\partial}{\partial x_j}\left[c_{p,j}\breve{f}_p^{(1)}\right]= -\frac{\partial}{\partial c_{p,i}}\left[\frac{(c_{p,i}-u_{f@p,i})}{\tau_p}\breve{f}_p^{(1)}\right]-\frac{\partial}{\partial\xi_p}\left[\frac{(\xi_p-t_{f@p})}{\tau_\theta}\breve{f}_p^{(1)}\right] \quad (1)$$

The first and the second terms on the right hand side (r.h.s) represent the effect of the external forces and heat exchanges acting on the particle respectively.

THE EULERIAN PARTICLE SPATIAL FILTERED EQUATIONS

Instantaneous moment transport equations are then derived from equation (1) by multiplying with functions ψ_p and integrating over the particle velocity and temperature spaces. Then, these equations are spatially filtered. Since particle number density is not homogenous, a Favre spatial filtering is used:

$$\bar{\bar{n}}_p\hat{\breve{\phi}}_p=\int G_{\Delta_f}(r)\breve{n}_p(x-r)\breve{\phi}_p(x-r)dr \quad (2)$$

where $G_{\Delta f}$ is the spatial filter kernel and Δ_f the characteristic length. In this work a spherical box filter, with the filter function $\frac{1}{\frac{\pi}{6}(\Delta_f)^3}H\left(\frac{1}{2}\Delta_f-|r|\right)$, is used.

A shortened version of the Euler LES system modeling the dispersed phase is:

$$\frac{\partial\bar{\bar{n}}_p}{\partial\tau}+\frac{\partial\bar{\bar{n}}_p\hat{\breve{u}}_{p,j}}{\partial x_j}=0 \quad (3)$$

$$\frac{\partial\bar{\bar{n}}_p\hat{\breve{u}}_{p,i}}{\partial\tau}+\frac{\partial\bar{\bar{n}}_p\hat{\breve{u}}_{p,j}\hat{\breve{u}}_{p,i}}{\partial x_j}=-\frac{\bar{\bar{n}}_p}{\bar{\bar{\tau}}_p}\left(\hat{\breve{u}}_{p,i}-\hat{u}_{f,i}\right)-\frac{\partial\bar{\bar{n}}_p\delta\hat{\breve{R}}^*_{p,ij}}{\partial x_j} -\frac{2}{3}\frac{\partial\bar{\bar{n}}_p\delta\hat{\breve{\theta}}_p\delta_{ij}}{\partial x_j}-\frac{\partial\Sigma_{p,ij}}{\partial x_j} \quad (4)$$

$$\frac{\partial\bar{\bar{n}}_pC_{pp}\hat{\breve{t}}_p}{\partial\tau}+\frac{\partial\bar{\bar{n}}_pC_{pp}\hat{\breve{u}}_{p,j}\hat{\breve{t}}_p}{\partial x_j}=-\frac{\bar{\bar{n}}_pC_{pp}}{\bar{\bar{\tau}}_\theta}\left(\hat{\breve{t}}_p-\hat{t}_f\right)-\frac{\partial\bar{\bar{n}}_pC_{pp}\delta\hat{\breve{\Theta}}_{p,j}}{\partial x_j} -\frac{\partial C_{pp}\Upsilon_{p,j}}{\partial x_j} \quad (5)$$

$$\frac{\partial\bar{\bar{n}}_p\delta\hat{\breve{\theta}}_p}{\partial\tau}+\frac{\partial\bar{\bar{n}}_p\hat{\breve{u}}_{p,j}\delta\hat{\breve{\theta}}_p}{\partial x_j}=-2\frac{\bar{\bar{n}}_p}{\bar{\bar{\tau}}_p}\delta\hat{\breve{\theta}}_p-\bar{\bar{n}}_p\delta\hat{\breve{R}}^*_{p,ij}\frac{\partial\hat{\breve{u}}_{p,i}}{\partial x_j} -\frac{2}{3}\bar{\bar{n}}_p\delta\hat{\breve{\theta}}_p\delta_{ij}\frac{\partial\hat{\breve{u}}_{p,i}}{\partial x_j}-\frac{1}{2}\frac{\partial\bar{\bar{n}}_p\delta\hat{\breve{Q}}_{p,iij}}{\partial x_j} -\frac{\partial\Psi_{p,j}}{\partial x_j}+\Pi_p \quad (6)$$

Copyright © 2008 by ASME

Downloaded From: https://proceedings.asmedigitalcollection.asme.org on 06/30/2019 Terms of Use: http://www.asme.org/about-asme/terms-of-use

All terms of the above equations are exacts with the exception of the terms of transfer in which mean particle relaxation times [23] are introduced as

$$\frac{1}{\overline{\overline{\tau}}_p} = \widehat{\left(\frac{1}{\tau_p}\right)}, \quad \frac{1}{\overline{\overline{\tau}}_\theta} = \widehat{\left(\frac{1}{\tau_\theta}\right)} \tag{7}$$

The dispersed phase is well characterized by the evolutions of the filtered particle number density (3), velocity (4) and temperature (5) while the filtered uncorrelated energy equation (6) is used to model the second order moment of Random Uncorrelated Motion (RUM). In the above equations, the filtered RUM tensor is already split into its deviatoric and spherical parts

$$\delta\hat{\overline{\overline{R}}}_{p,ij} = \delta\hat{\overline{\overline{R}}}^*_{p,ij} + \frac{1}{3}\delta\hat{\overline{\overline{R}}}_{p,kk}\delta_{ij} = \delta\hat{\overline{\overline{R}}}^*_{p,ij} + \frac{2}{3}\delta\hat{\overline{\overline{\theta}}}_p\delta_{ij} \tag{8}$$

The physical signification of the r.h.s terms of the above particle equations are explained below.

Filtered correlated velocity $\hat{\overline{\overline{u}}}_{p,i}$ transport equation (4):

- the first term represents the momentum transfer through the drag force;
- the second and the third terms are the contributions of the uncorrelated velocity correlations and are analogous to the viscous and pressure contributions in the carrier flow equations, respectively ;
- the fourth term represents the contribution of the subgrid correlated motions. The mesoscopic subgrid stress tensor is defined as

$$\Sigma_{p,ij} = \overline{\overline{n}}_p\left(\widehat{\bar{u}_{p,i}\bar{u}_{p,j}} - \hat{\bar{u}}_{p,i}\hat{\bar{u}}_{p,j}\right) \tag{9}$$

Filtered correlated temperature $\hat{\overline{\overline{t}}}_p$ transport equation (5):

- the first term represents the heat transfer by interaction with the carrier fluid;
- the second term is the contribution of the Random Uncorrelated Heat Flux (RUHF) on the correlated temperature;
- the third one represents the contribution of the subgrid correlated motions. The mesoscopic subgrid heat flux is defined as

$$\Upsilon_{p,i} = \overline{\overline{n}}_p\left(\widehat{\bar{u}_{p,i}\bar{t}_p} - \hat{\bar{u}}_{p,i}\hat{\bar{t}}_p\right) \tag{10}$$

Filtered Quasi-Brownian energy $\delta\hat{\overline{\overline{\theta}}}_p$ transport equation (6):

- the first term represents the dissipation of the QB energy by drag with carrier flow;
- the second and the third ones represent the production of QB energy by shear and compression respectively;
- the fourth term is the diffusion of QB energy;
- the fifth term represents the subgrid diffusion and it is defined as

$$\Psi_{p,i} = \overline{\overline{n}}_p\left(\widehat{\bar{u}_{p,i}\delta\bar{\theta}_p} - \bar{u}_{p,i}\delta\bar{\theta}_p\right) \tag{11}$$

- the sixth one represents the subgrid production of QB energy and it is

$$\Pi_p = -\overline{\overline{n}}_p\left(\widehat{\delta\bar{R}_{p,ij}\frac{\partial\bar{u}_{p,i}}{\partial x_j}} - \delta\hat{\bar{R}}_{p,ij}\frac{\partial\hat{\bar{u}}_{p,i}}{\partial x_j}\right) \tag{12}$$

In the LES particle system, all moments of the Quasi-Brownian velocity and temperature must to be modeled as well as all subgrid terms. In the following paragraphs, both closures are presented.

RANDOM UNCORRELATED MOMENTS MODELING

A viscosity model (Simonin et al. [8]) is used for the deviatoric part of filtered RUM tensor

$$\begin{aligned}\delta\hat{\overline{\overline{R}}}^*_{p,ij} &= \nu_{QB}\,2\hat{\overline{\overline{S}}}^*_{p,ij} \\ &= -\frac{\overline{\overline{\tau}}_p}{3}\delta\hat{\overline{\overline{\theta}}}_p\left[\frac{\partial\hat{\bar{u}}_{p,i}}{\partial x_j} + \frac{\partial\hat{\bar{u}}_{p,j}}{\partial x_i} - \frac{2}{3}\frac{\partial\hat{\bar{u}}_{p,k}}{\partial x_k}\delta_{ij}\right]\end{aligned} \tag{13}$$

while a diffusivity law, suggested by Kaufmann et al. [9] is retained to model contracted third order moment of uncorrelated motion

$$\frac{1}{2}\delta\hat{\overline{\overline{Q}}}_{p,iij} = -\frac{5}{3}\overline{\overline{\tau}}_p\delta\hat{\overline{\overline{\theta}}}_p\frac{\partial\delta\hat{\overline{\overline{\theta}}}_p}{\partial x_j} \quad . \tag{14}$$

In order to close the RUHF, a gradient equilibrium model issued from the second order moment (QB heat flux) transport equation is proposed. It leads to

$$\delta\hat{\overline{\overline{\Theta}}}_{p,i} = -\frac{2}{3}\left(\frac{\overline{\overline{\tau}}_p\overline{\overline{\tau}}_\theta}{\overline{\overline{\tau}}_p + \overline{\overline{\tau}}_\theta}\right)\delta\hat{\overline{\overline{\theta}}}_p\frac{\partial\hat{\overline{\overline{t}}}_p}{\partial x_j}. \tag{15}$$

The equilibrium assumption is considered only to supply a first simple modelling. However, such assumption remains very questionable for inertial particles [9].

SUBGRID-SCALES (SGS) MODELING

The subgrid stress tensor $\Sigma_{p,ij}$ is split into deviatoric and spherical parts and a Smagorinsky-type and a Yoshizawa-type models are used to represent the anisotropic SGS stresses and the subgrid energy, respectively (see Moin *et al.* [10] or Lenormand *et al.* [22] for single-phase and Moreau *et al.* [6,24] for two-phase flows). The modeled tensor is then

$$\begin{aligned}\Sigma_{p,ij} &= \Sigma^*_{p,ij} + \frac{1}{3}\Sigma_{p,kk}\delta_{ij} \\ &= -2\overline{\overline{n}}_p C_S{}^2\Delta_f{}^2\left|\hat{\overline{\overline{S}}}^*_p\right|\hat{\overline{\overline{S}}}^*_{p,ij} + \frac{2}{3}\overline{\overline{n}}_p C_Y\Delta_f{}^2\left|\hat{\overline{\overline{S}}}^*_p\right|^2\end{aligned} \tag{16}$$

where the filtered particle rate-of-strain tensor and its norm are

$$\hat{\overline{\overline{S}}}^*_{p,ij} = \frac{1}{2}\left(\frac{\partial\hat{\bar{u}}_{p,i}}{\partial x_j} + \frac{\partial\hat{\bar{u}}_{p,j}}{\partial x_i} - \frac{2}{3}\frac{\partial\hat{\bar{u}}_{p,k}}{\partial x_k}\delta_{ij}\right) \text{ and } \left|\hat{\overline{\overline{S}}}^*_p\right|^2 = \left(2\hat{\overline{\overline{S}}}^*_{p,ij}\hat{\overline{\overline{S}}}^*_{p,ij}\right)$$

Copyright © 2008 by ASME

Downloaded From: https://proceedings.asmedigitalcollection.asme.org on 06/30/2019 Terms of Use: http://www.asme.org/about-asme/terms-of-use

This model uses a linear eddy-viscosity assumption in which the energy is always transferred from filtered to residual motion, thus, no backscatter phenomenon is predicted. Moreover, it is well-know that it overestimates the dissipation rate in the laminar-turbulent transition region. A good alternative seems to be given by a mixed model, proposed by Speziale *et al.* [11], obtained from Leonard's triple decomposition, in which the effects of momentum exchange between small and large scales are accounted for by the Leonard and Cross terms. The decomposition, based on Favre filtering, lead to a Leonard-stress tensor (not modeled), a Cross-stress tensor modeled by a scale-similarity assumption (Bardina *et al.* [12]) with a model coefficient of unity imposed to ensure Galilean invariance, and a Reynolds-stress tensor that, split in deviatoric and isotropic parts can be modeled by Smagorinsky and Yoshizawa models respectively (see for instance Erlebacher *et al.* [13]).

Adapted to the mesoscopic flows [6,24], the mixed model leads to

$$\Sigma_{p,ij} = \overline{\overline{n}}_p(\widehat{\hat{\tilde{u}}_{p,i}\hat{\tilde{u}}_{p,j}} - \hat{\tilde{\tilde{u}}}_{p,i}\hat{\tilde{\tilde{u}}}_{p,j}) - 2\overline{\overline{n}}_p C_S'\Delta_f{}^2\left|\hat{\tilde{S}}^*{}_p\right|\hat{\tilde{S}}^*{}_{p,ij} + \frac{2}{3}\overline{\overline{n}}_p C_Y'\Delta_f{}^2\left|\hat{\tilde{S}}^*{}_p\right|^2 \quad (17)$$

Analogously, we propose to extend a classical eddy-diffusivity type (see, for instance, Martin *et al.* [14] for single-phase description) at the dispersed phase in order to model the mesoscopic SGS heat flux, which takes the form:

$$\mathrm{Y}_{p,j} = \frac{\overline{\overline{n}}_p C_S{}^2\Delta_f{}^2\left|\hat{\tilde{S}}^*{}_p\right|}{\mathrm{Pr}_T}\frac{\partial\hat{\tilde{t}}_p}{\partial x_j} \quad (18)$$

where C_S is the Smagorinsky coefficient and Pr_T is the turbulent Prandtl number that has to be fixed or calculated dynamically (as suggested by Martin *et al.* [14]). In this model, similarly to the Smagorinsky type, a linear eddy-viscosity is used with a mixing length hypothesis (the length scale is proportional to the filter width). This is the simplest approach to model the mesoscopic subgrid heat flux. Also in this case, a mixed model proposed originally by Speziale *et al.* [11], can be adapted to dispersed phase. It becomes:

$$\mathrm{Y}_{p,j} = -\frac{\overline{\overline{n}}_p C_S'\Delta_f{}^2\left|\hat{\tilde{S}}^*{}_p\right|}{\mathrm{Pr}_T}\frac{\partial\hat{\tilde{t}}_p}{\partial x_j} + \overline{\overline{n}}_p(\widehat{\hat{\tilde{u}}_{p,j}\hat{\tilde{t}}_p} - \hat{\tilde{\tilde{u}}}_{p,j}\hat{\tilde{\tilde{t}}}_p) \quad (19)$$

A simple eddy-diffusivity model (Moin *et al.* [10]) and a more accurate mixed model (Speziale *et al.* [11]), both adapted [6], are used to model the subgrid diffusion. The first leads to

$$\Psi_{p,j} = -\frac{\overline{\overline{n}}_p C_S{}^2\Delta_f{}^2\left|\hat{\tilde{S}}^*{}_p\right|}{\mathrm{Pr}_T}\frac{\partial\delta\hat{\tilde{\theta}}_p}{\partial x_j} \quad (20)$$

while the second leads to

$$\Psi_{p,j} = -\frac{\overline{\overline{n}}_p C_S{}^2\Delta_f{}^2\left|\hat{\tilde{S}}^*{}_p\right|}{\mathrm{Pr}_T}\frac{\partial\delta\hat{\tilde{\theta}}_p}{\partial x_j} + \overline{\overline{n}}_p(\widehat{\hat{\tilde{u}}_{p,i}\delta\hat{\tilde{\theta}}_p} - \hat{\tilde{\tilde{u}}}_{p,i}\delta\hat{\tilde{\tilde{\theta}}}_p) \quad (21)$$

Finally, in order to model Quasi-Brownian sub-grid production, Moreau [6] proposed a Ghosal-type model (Ghosal *et al.* [15]) where the production term is computed by using subgrid correlated energy evaluated by a Yoshizawa or scale-similarity-type model. It can be written as:

$$\Pi_p = C\frac{\overline{\overline{n}}_p q_{p,SGS}^{3/2}}{\Delta_f} \quad (22)$$

where $q_{p,SGS} = \frac{1}{3}\Sigma_{p,kk}\delta_{ij}$ is the subgrid energy and C is a constant which can be calculated under assumption of a global equilibrium in a homogenous direction (Vreman [16]).

NUMERICAL SIMULATION

Our numerical simulation corresponds to the dispersion of a cold particle-laden planar turbulent jet. The initial velocity and temperature profiles of the carrier phase are imposed as hyperbolic tangent types supplemented with statistically homogeneous and isotropic velocity fluctuations. Particles are randomly embedded at the same velocity and temperature of the carrier flow and their number is large enough to permit Mesoscopic fields calculation. The numerical simulation is performed by a Lagrangian approach (DPS) coupled with a DNS of the carrier flow. The code used is the Euler-Lagrange NTMIX3D-2Φ which solves the compressible Navier-Stokes and energy equations in the dimensionless form with a third order Runge-Kutta time stepping and a sixth order compact finite difference scheme on cartesian grid. Also the advancement in time in Lagrangian tracking is ensured by a third order Runge-Kutta scheme. The interpolation of the Eulerian carrier flow variables at the location of the particles is performed by a third order Lagrange polynomial algorithm. The simulation domain is a cube with periodic boundary conditions. The principal parameters are listed in table 1.

Lagrangian equations used in the DPS and governing the motion and heat exchange of each particle are:

$$\frac{d\mathbf{X}_p{}^{(k)}(\tau)}{d\tau} = \mathbf{V}_p{}^{(k)}(\tau), \quad (23)$$

$$\frac{d\mathbf{V}_p{}^{(k)}(\tau)}{d\tau} = -\frac{1}{\tau_p}(\mathbf{V}_p{}^{(k)} - \mathbf{u}_{f@p}), \quad (24)$$

$$\frac{dT_p{}^{(k)}(\tau)}{d\tau} = -\frac{1}{\tau_\theta}(T_p{}^{(k)} - t_{f@p}), \quad (25)$$

where $\mathbf{u}_{f@p}$ and $t_{f@p}$ are the undisturbed fluid velocity and temperature at the particle location, and τ_p et τ_θ are the dynamical and thermal relaxation times respectively defined as

$$\tau_p = \frac{4\rho_p d_p}{3\rho_f C_D\left\|\mathbf{V}^{(k)} - \mathbf{u}_{f@p}\right\|} \quad \text{and} \quad \tau_\theta = \frac{1}{6}\frac{\mathrm{Pr}\, d_p{}^2 C_{pp}\rho_p}{Nu\mu C_p} \quad (26)$$

with the drag coefficient and the Nusselt number

Copyright © 2008 by ASME

Downloaded From: https://proceedings.asmedigitalcollection.asme.org on 06/30/2019 Terms of Use: http://www.asme.org/about-asme/terms-of-use

$$C_D = \frac{24}{\mathrm{Re}_p}(1 + 0.15\,\mathrm{Re}_p^{\,0.687}),\ Nu = 2 + 0.55\,\mathrm{Re}_p^{\,0.5}\,\mathrm{Pr}^{0.33} \quad (27)$$

formulated in term of the particle Reynolds number

$$\mathrm{Re}_p = \frac{\left\|\mathbf{V}^{(k)} - \mathbf{u}_{f@p}\right\| d_p}{\upsilon}. \quad (28)$$

Pr is the Prandtl number while C_p and C_{pp} are the specific heat at constant pressure of fluid and particles.

Parameters	Value
Box size L	2π
Number of cells	128^3
Size of cells Δx^3	0.049^3
Kinematics Viscosity ν	1.82e-4
Initial turbulent kinetic energy q^2_f	3.37e-4
Initial dissipation ε_f	3.78e-5
Jet mean velocity U_0	0.15
Jet mean temperature T_0	2.0
External mean temperature T_∞	2.5
Prandtl number	0.7
Planar jet initial width	1.6
Total particle number	$80x10^6$
Dynamics relaxation time τ_p on y=0	12.8
Dynamics Stokes number St (estimate at the equilibrium) on y=0	~0.9
Thermal relaxation time τ_θ on y=0	26
Thermal Stokes number St_T (estimate at the equilibrium) on y=0	~1.8

Table 1: simulation parameters

Lagrangian values are then post-processed and mesoscopic fields are computed by using a projection algorithm [6,24]. Δ_p is the characteristic size of projection mesh chosen as that $\Delta_p = \Delta x$. In order to estimate the dynamical and thermal Stokes numbers, the particle fluctuation energy is supposed at the equilibrium with the turbulence of carrier flow (Tchen hypothesis) for the velocity components in spanwise direction (Simonin [17]). Previous assumption allows to calculate an effective Stokes number defined as the ratio between the particle relaxation time and a time scale characteristic of turbulence seen by the particles $St = \tau_p / \tau^+_f$. When the dynamical Stokes number is found, the characteristic time scale τ^+_f is estimated and, finally, the thermal Stokes number $St_T = \tau_\theta / \tau^+_f$ is computed. Figure 1 shows a snapshot corresponding to the particle density time evolution. As can be seen from the figure, the Stokes number *St* corresponds to a regime of preferential concentration. Figure 2 shows the averaged profiles of mesoscopic velocity and temperature of the dispersed phase against the corresponding fluid fields, for a fixed time. Figure 3 shows the averaged profile of the particle number density and the profiles of the Stokes numbers, at fixed time. The averages are computed over planes parallel to the stream direction.

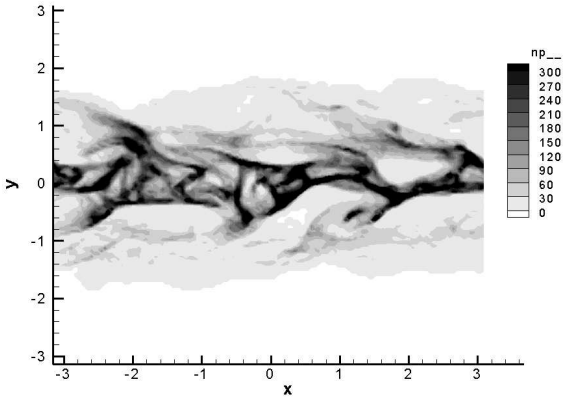

Figure 1: *snapshot on Z=64 of* $\breve{n}_p$ *at time* $\tau = 4.8\,\tau^+_f$

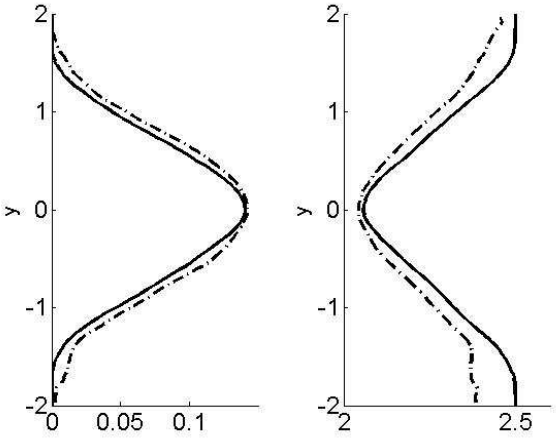

Figure 2: *averaged profiles of velocity (left) and temperature (right) at time* $\tau = 4.8\,\tau^+_f$*; fluid (–), particles (–.–) .*

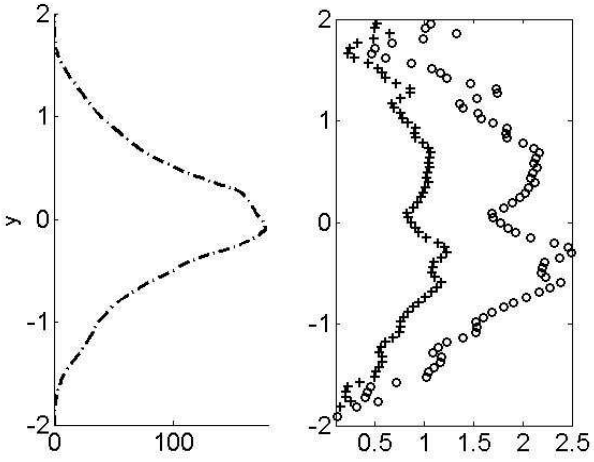

Figure 3: *averaged profiles of particle number density* $\breve{n}_p$ *(left) and Stokes numbers (right), dynamical St (+) and thermal* St_T *(o), at time* $\tau = 4.8\,\tau^+_f$.

Copyright © 2008 by ASME

Downloaded From: https://proceedings.asmedigitalcollection.asme.org on 06/30/2019 Terms of Use: http://www.asme.org/about-asme/terms-of-use

NUMERICAL SIMULATION VERSUS MODELING: A PRIORI TESTING

In this paragraph the results of *a priori* tests are presented. The evaluation of the model accuracy is made comparing the exact terms against the modeled by using correlation coefficients defined by [18]

$$c(A,B)=\frac{\langle AB\rangle-\langle A\rangle\langle B\rangle}{\sqrt{\left(\langle A^2\rangle-\langle A\rangle^2\right)\left(\langle B^2\rangle-\langle B\rangle^2\right)}} \qquad (29)$$

The model reproducing exactly real term give correlation coefficient equal to 1. The angle brackets denote average over planes parallel to the stream direction.

Random uncorrelated moments modeling

The evolutions in time of correlation coefficients issued from *a priori* tests on random uncorrelated moments are shown. The time axis was made dimensionless using the characteristic time scale t_f^t. Results in the figures correspond to values computed on the plane y=0.68. This plane is close to periphery of jet in the initial configuration. In order to test viscosity model for the RUM tensor (equation 13), correlation coefficients of the exact term against its model for the dissipation of mesoscopic kinetic energy $\overline{\overline{n}}_p \delta\hat{\hat{R}}^*_{p,ij}\frac{\partial \hat{\hat{u}}_{p,i}}{\partial x_j}$ are calculated and plotted on Figure 4. The tests found correlation coefficients greater than 0.8 confirming the assumption of the alignment between filtered second order uncorrelated motion and filtered rate of strain tensor. Same tests performed for the RUHF modeling (equation 15) are displayed on figure 5. The correlation coefficients are calculated in term of dissipation of mesoscopic temperature variance $\overline{\overline{n}}_p \delta\hat{\hat{\Theta}}_{p,j}\frac{\partial \hat{\hat{t}}_p}{\partial x_j}$. Also this model shows a good behavior.

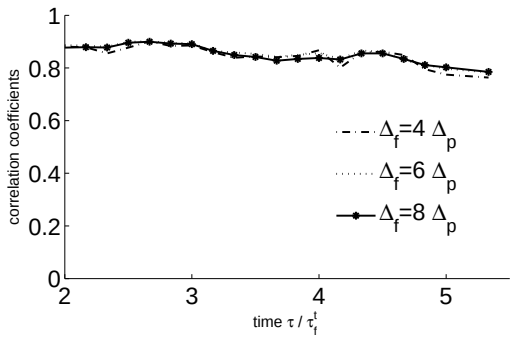

Figure 4: *correlation coefficient for contracted RUM tensor; y=0.68.*

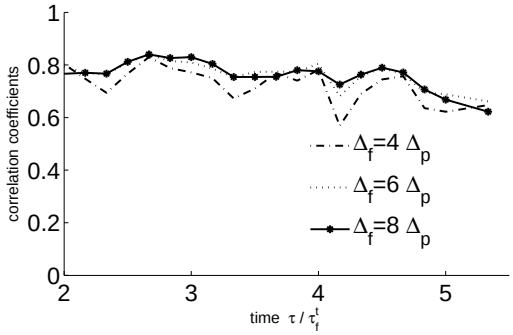

Figure 5: *correlation coefficient for contracted RUHF; y=0.68.*

In the other hand, these models are not able to predict positive values of dissipation. Such behavior is clearly visible on figures 6 and 7 where the p.d.f. of the contracted RUM tensor and RUHF are plotted respectively. For dispersed phase, positive values mean that local phenomena of transfer from uncorrelated to correlated motions can occur. The probability to have positive values increases with inertia of particles [6].

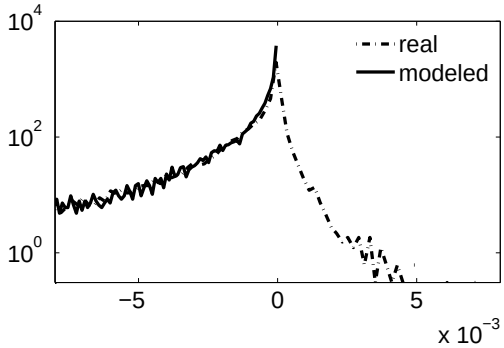

Figure 6: *p.d.f. of contracted RUM tensor at time* $\tau=4.8\,t_f^t$ *for* $\Delta_f = 4\Delta_p$

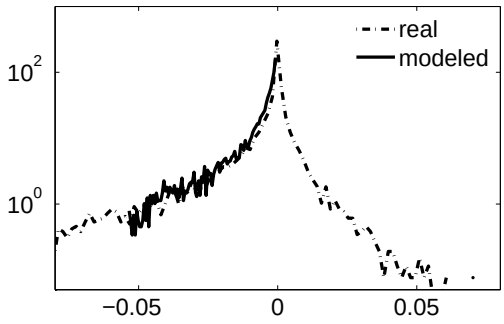

Figure 7: *p.d.f. of contracted RUHF at time* $\tau=4.8\,t_f^t$ *for* $\Delta_f = 4\Delta_p$

Unfortunately, the diffusivity model (equation 14) for the third order contracted uncorrelated moment, do not give satisfactory results.

Copyright © 2008 by ASME

Downloaded From: https://proceedings.asmedigitalcollection.asme.org on 06/30/2019 Terms of Use: http://www.asme.org/about-asme/terms-of-use

SGS terms modeling

In this section the results of a priori testing on the SGS models are presented. As in previous tests, the results are shown for the plane of coordinate y=0.68. On Figure 8, the comparison between the exact term against the Smagorinsky and mixed model (deviatoric part of equations 16-17) is displayed in term of subgrid dissipation of correlated kinetic energy $\Sigma^*_{p,ij}\frac{\partial\hat{\tilde{u}}_{p,i}}{\partial x_j}$ (contracted SGS stresses). As expected, the mixed model gives coefficient values higher than the Smagorinsky ones. A similar behavior is found for the subgrid energy (see figure 9) comparing the Yoshizawa and the mixed model (isotropic part of equations 16-17).

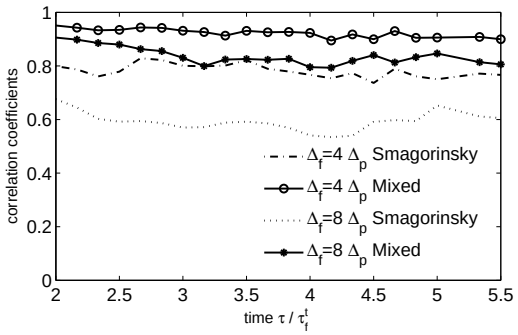

Figure 8: *correlation coefficient for contracted SGS stresses; y=0.68.*

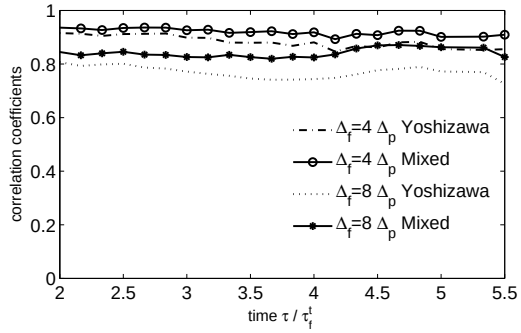

Figure 9: *correlation coefficient for SGS energy; y=0.68.*

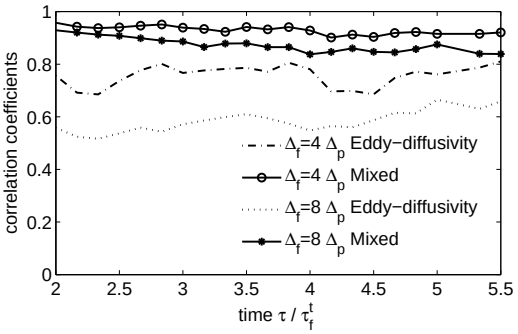

Figure 10: *correlation coefficient for contracted SGS heat flux; y=0.68.*

The SGS heat flux is tested under its contracted form $Y_{p,j}\frac{\partial\hat{\tilde{t}}_p}{\partial x_j}$, and the results are displayed on figure 10. As for the SGS stresses and energy, the mixed model (equation 19) gives better results than the eddy-diffusivity type (equation 18).

To check the differences between mixed and gradient like models, the profiles of the correlation coefficients across the jet at a fixed time are computed. The results for the contracted SGS stresses and the contracted SGS heat flux are displayed on figure 11 and 12 respectively. The mixed models confirm better accuracy also in term of spatial location values.

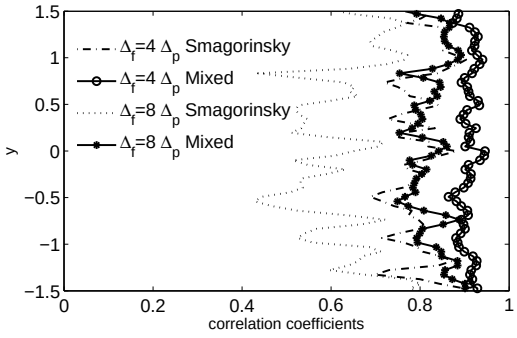

Figure 11: *correlation coefficient for contracted SGS stresses; τ=4.8τ_f^t.*

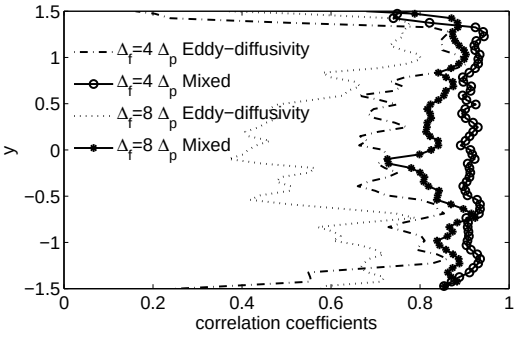

Figure 12: *correlation coefficient for contracted SGS heat flux; τ=4.8τ_f^t.*

On Figure 13, the results of *a priori* tests for the subgrid Quasi-Brownian diffusion in term of contracted diffusion $\frac{\partial\Psi_{p,j}}{\partial x_j}$ for the eddy-diffusivity and mixed model (equation 20-21) are shown.

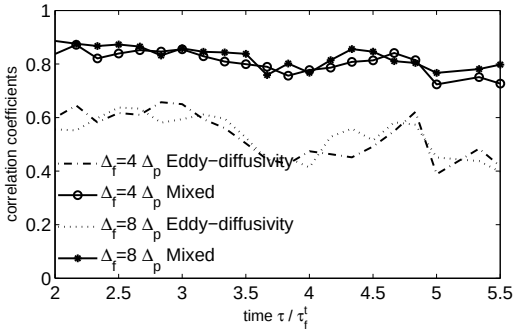

Figure 13: *correlation coefficient for contracted SGS diffusion; y=0.68.*

Copyright © 2008 by ASME

Downloaded From: https://proceedings.asmedigitalcollection.asme.org on 06/30/2019 Terms of Use: http://www.asme.org/about-asme/terms-of-use

Also in this case the mixed model behaves better than the eddy diffusivity one.

The last term tested is the subgrid Quasi-Brownian production (equation 22). The Ghosal-type model gives coefficient values in the range of 0.2 and 0.4 (results not shown).

To conclude on the SGS modeling, models using assumption as the rate-of-strain tensor or gradient alignment (as Smagorinsky type) give satisfactory results in term of scalar correlation coefficients. But such models are not able to predict phenomena as the transfer from smaller to larger scales as predicted by the mixed models. To illustrate this behavior, figures 14 and 15 show the p.d.f. of the real against modeled mesoscopic subgrid heat flux for the eddy-diffusivity and the mixed model respectively.

In the case of mixed models, where a scale similarity assumption is added, results shown a very good behavior confirming their better accuracy.

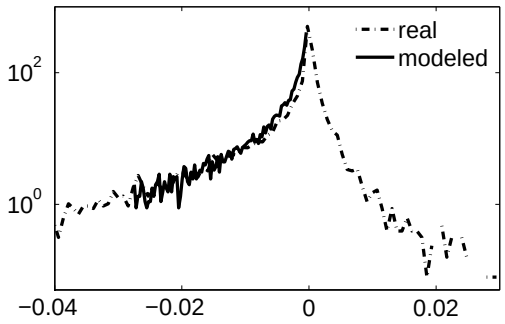

Figure 14: *p.d.f. of contracted SGS heat flux at time* $\tau=4.8\,\tau_f^t$ *for* $\Delta_f = 4\Delta_p$*; eddy -diffusivity model.*

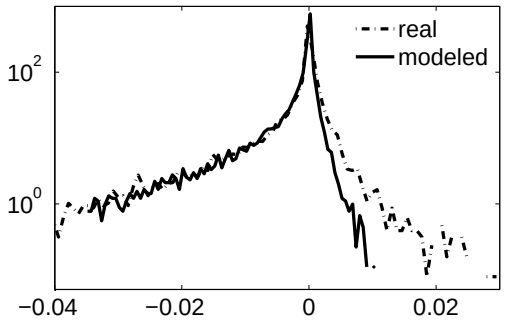

Figure 15: *p.d.f. of contracted SGS heat flux at time* $\tau=4.8\,\tau_f^t$ *for* $\Delta_f = 4\Delta_p$*; mixed model.*

SGS model constants

The correlation coefficient values are independent of the constant used in the different models (they are invariant to the additive or multiplicative constants). In order to evaluate the model coefficients, the models are computed without constants and the constants are calculated as the ratio between the exact and the modeled terms, both averaged on planes parallel to the stream direction. This procedure is applied on scalar level and the scalar quantities are achieved for tensor or vector variables by contracted them. Figures 16 and 17 display the Smagorinsky coefficient C_S versus time and cross-stream coordinates. On Figures 18 and 19, the results for the Yoshizawa constant C_Y are shown.

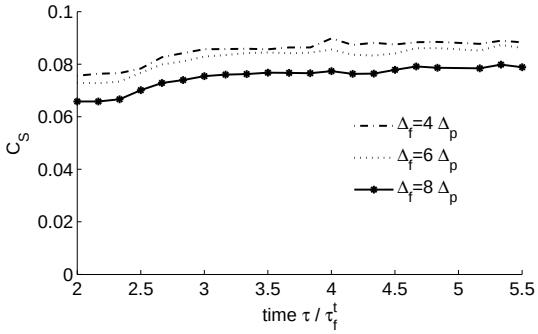

Figure 16: *Smagorinsky constant; y=0.68.*

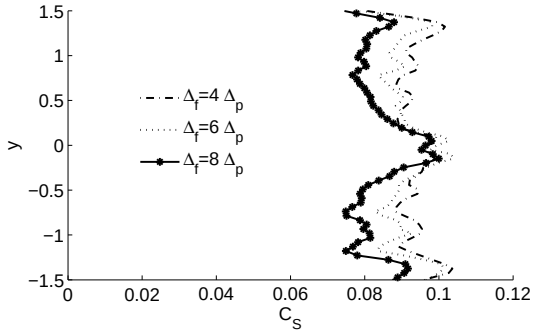

Figure 17: *Smagorinsky constant;* $\tau=4.8\,\tau_f^t$.

The values of C_S are mainly included between 0.08 and 0.1, quit comparables to the classical values found for the shear turbulent flows (Deardoff [19]: 0.1 in turbulent channel with filter width equal to grid size).

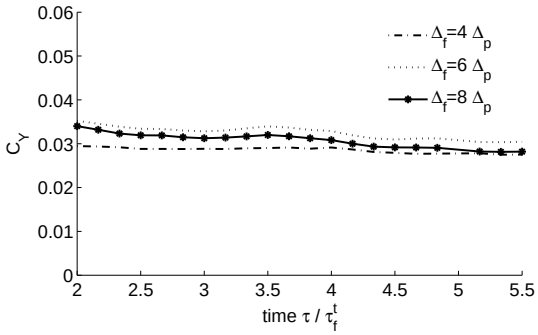

Figure 18: *Yoshizawa constant; y=0.68.*

The values of C_Y vary between 0.03 and 0.04 and they seem smaller than theoretical value for single-phase flow (see Yoshizawa [20] or Martin *et al.* [14] which give value ~0.09).

Copyright © 2008 by ASME

Downloaded From: https://proceedings.asmedigitalcollection.asme.org on 06/30/2019 Terms of Use: http://www.asme.org/about-asme/terms-of-use

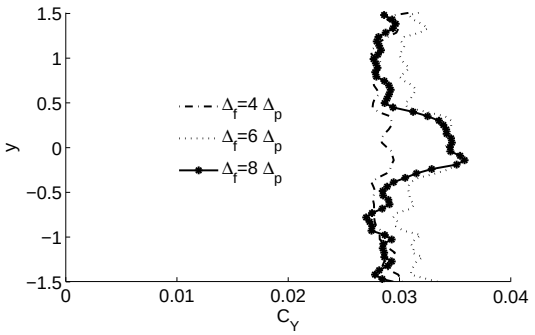

Figure 19: *Yoshizawa constant;* $\tau=4.8\tau_f^t$.

About the mixed model, the values of constant C'_S range between 0.003 and 0.006 and those of C'_Y between 0.012 and 0.02. We notice that correspondent values for compressible single-phase flows are C'_S=0.0085 and C'_Y=0.0033 (Zang *et al.* [21], Erlebacher *et al*. [13] where the constants are divided for $\sqrt{2}$ and 2 respectively to have comparable values). The values of C'_S seem to be lower than the single-phase one, while the values of C'_Y are found much greater than the single-phase reference. In the compressible single-phase flows, when a dynamical model is used to evaluate C'_Y, studies shown that in some case its value is higher than that predicted by the theory (see for instance Moin *et al*. [10]). Other studies [13,21] pointed out the insensitivity of the LES results to the value of this constant for turbulent Mach numbers <0.4. In case of the dispersed phase where the Mach number is largely greater then 1 (when an equivalent speed of sound [7] is used), this point should be further investigated and dependencies evaluated. Also a dynamical adjustment of the model coefficients should be tested [14].Imposing the found constants, a turbulent Prandtl number Pr_T included between 0.65 and 0.85 is computed. In conclusion, about the evaluation of the above model coefficients, since several studies shown that they are subjected to variability with the grid resolution and the energy spectrum [10] and also with the evaluation method, in tensor, vector and scalar level [13], further studies should be made.

CONCLUSION

In this paper a set of Eulerian filtered equations for the dispersed phase in a non isothermal configuration are presented. The system of local and instantaneous filtered equations is derived by using of Mesoscopic Eulerian Formalism extended to the temperature. The unclosed terms issued from the statistical approach (random uncorrelated moments) are closed by an equilibrium assumption. The subgrid terms issued from the spatial filtering are closed adapting classical compressible models to the dispersed phase. System and models are validates by *a priori* tests and results are found globally satisfactory. As further work, model coefficients should be better investigated. The results are found promising in order to accomplish real Euler-Euler Large-Eddy Simulations and to validate the model by using *a posteriori* tests.

ACKNOWLEDGMENTS

This work received funding from the European Community through the project TIMECOP-AE (Project # AST5-CT-2006-030828). It reflects only the author's views and the Community is not liable for any use that may be made of the information contained therein. Numerical simulations were performed on the IBM Power4 machine. Support of Institut de Développment et des Ressources en Informatique Scientifique (IDRIS) is gratefully acknowledged.

REFERENCES

[1] P. Février, O. Simonin, K.D. Squires, *J. Fluid Mech.*, 533 (2005), 1.
[2] Q. Wang, K. D. Squires, *Phys. Fluids*, 8 (1996), 1207.
[3] M. Boivin, O. Simonin, *Physics of Fluids*, 12 (2000), 2080.
[4] Y. Yamamoto, M. Potthoff, T. Tanaka, T. Kajishima, Y. Tsuji, *J. Fluid Mech.*, 442 (2001), 303.
[5] P. Fede, O. Simonin, *Physics of Fluids*, 18 (2006), 1.
[6] M. Moreau, *PhD thesis*, INP Toulouse (2006).
[7] A. Kaufmann, *PhD thesis*, CERFACS Toulouse (2004).
[8] O. Simonin, P. Février, J. Laviéville, *J. of Turbulence*, 3 (2002) 1.
[9] A. Kaufmann, M. Moreau, O. Simonin, J. Helie, *J. Comp. Physics*, preprint submitted (2008).
[10] P. Moin, K. Squires, W. Cabot, S. Lee, *Physics Fluids A*, 3 (1991), 2746.
[11] C. G. Speziale, G. Erlebacher, T. A. Zang, M. Y. Hussaini, *Physics of Fluids*, 31 (1998), 940.
[12] J. Bardina, J. H. Ferziger, W. C. Reynolds, *AIAA*, 80 (1980)-1357
[13] G. Erlebacher, M. Y. Hussaini, C. G. Speziale, T. A. Zang, *J. Fluid Mech.*, 238 (1992), 155.
[14] M. P. Martin, U. Piomelli, G. V. Candler, *Theoret. Comput. Fluid Dynamics*, 13 (2000), 361.
[15] S. Ghosal, T. S. Lund, P. Moin, K. Akselvoll, *J. Fluid Mech.*, 286 (1995), 1760.
[16] B. Vreman, B. Geurts, H. Kuerten, *Int. J. Numer. Methods Fluids*, 22 (1996), 297.
[17] O. Simonin, *Proc. 4th Intl Symp. on Gas-Solid Flows*, ASME FED, 121 (1991), 197.
[18] M. V. Salvetti, S. Banerjee, *Physics of Fluids*, 7 (1994), 2831.
[19] J. W. Deardorff, *J. Fluids Eng.*, 95 (1973), 429.
[20] A. Yoshizawa, *Phys. Fluids*, 29 (1986), 2152.
[21] T. A. Zang, R. B. Dahlburg, J. P. Dahlburg , *Physics Fluids A*, 4 (1992), 127.
[22] E. Lenormand, P. Sagaut, L. Ta Phuoc, *Int. J. Numer. Meth. Fluids*, 32 (2000), 369-406.
[23] O. Simonin, in *Lecture Series 2000-06*, VKI for Fluid Dynamics (2000).
[24] M. Moreau, B. Bédat, O. Simonin, *ILASS Americas 18th Annual Conference, Irvine, CA* (2005).

Copyright © 2008 by ASME

Downloaded From: https://proceedings.asmedigitalcollection.asme.org on 06/30/2019 Terms of Use: http://www.asme.org/about-asme/terms-of-use

APPENDIX A

MESOSCOPIC EULERIAN FORMALISM EXTENDED TO THE TEMPERATURE

Dispersed phase can be statistically described by one-particle probability function (p.d.f.) obtained by ensemble averaging over a very large number $\mathcal{N}_{f\&p}$ of two-phase flow realisations $\mathcal{H}_{f\&p}$. However, this approach loose information concerning spatial or temporal velocity correlation between particles so, to overcome this limit, MEF ([1]), propose to characterize statistically for dispersed phase associated to one realisation of fluid $\mathcal{H}_f$. One can envision a large number $\mathcal{N}_p$ of particulate phase realisations $\mathcal{H}_p$ which differ slightly, from a macroscopic point of view, in the initial conditions. By an ensemble average applied on the $\mathcal{N}_p$ realisation $\mathcal{H}_p$ conditioned to the flow realisation $\mathcal{H}_f$, to the refined-grid function $W_p^{(m)}$ describing a single particle m in phase space,

$$W_p^{(m)}(\mathbf{x},\mathbf{c}_p,\xi_p,\tau\left|\mathcal{H}_p,\mathcal{H}_f\right.)=\delta(\mathbf{x}-\mathbf{x}_p^{(m)}(\tau))\delta(\mathbf{c}_p-\mathbf{v}_p^{(m)}(\tau))\delta(\xi_p-t_p^{(m)}(\tau))$$

one can define the p.d.f. representing the average number of particle centres at the position $\mathbf{x}$, with a given velocity $\mathbf{v}_p^{(m)}(\tau)=\mathbf{c}_p$ and temperature $t_p^{(m)}(\tau)=\xi_p$ at time τ:

$$\breve{f}_p^{(1)}(\mathbf{x},\mathbf{c}_p,\xi_p,\tau,\mathcal{H}_f)=\lim_{\mathcal{N}_p\to\infty}\left[\frac{1}{\mathcal{N}_p}\sum_{\mathcal{N}_p}\sum_{m=1}^{N_p}W_p^{(m)}(\mathbf{x},\mathbf{c}_p,\xi_p,\tau,\left|\mathcal{H}_p,\mathcal{H}_f\right.)\right] \quad \text{(A1)}$$

The associated moments are, in order, local and instantaneous particle number density, mesoscopic velocity and mesoscopic temperature:

$$\breve{n}_p(\mathbf{x},\tau,\mathcal{H}_f)=\int\breve{f}_p^{(1)}(\mathbf{x},\mathbf{c}_p,\xi_p,\tau,\mathcal{H}_f)d\mathbf{c}_p d\xi_p \quad \text{(A2)}$$

$$\breve{v}_{p,i}(\mathbf{x},\tau,\mathcal{H}_f)=\frac{1}{\breve{n}_p(\mathbf{x},\tau,\mathcal{H}_f)}\int c_{p,i}\breve{f}_p^{(1)}(\mathbf{x},\mathbf{c}_p,\xi_p,\tau,\mathcal{H}_f)d\mathbf{c}_p d\xi_p \quad \text{(A3)}$$

$$\breve{t}_p(\mathbf{x},\tau,\mathcal{H}_f)=\frac{1}{\breve{n}_p(\mathbf{x},\tau,\mathcal{H}_f)}\int\xi_p\breve{f}_p^{(1)}(\mathbf{x},\mathbf{c}_p,\xi_p,\tau,\mathcal{H}_f)d\mathbf{c}_p d\xi_p \quad \text{(A4)}$$

For a given realisation $\mathcal{H}_f$, velocity and temperature can be formally written in terms of an instantaneous Eulerian mesoscopic field and a residual contribution associated with each particle and defined along its trajectory

$$\mathbf{v}_p^{(m)}(\tau)=\breve{\mathbf{v}}_p(\mathbf{x}_p^{(m)}(\tau),\tau,\mathcal{H}_f)+\delta\mathbf{v}_p^{(m)}(\tau) \quad \text{(A5)}$$

$$t_p^{(m)}(\tau)=\breve{t}_p(\mathbf{x}_p^{(m)}(\tau),\tau,\mathcal{H}_f)+\delta t_p^{(m)}(\tau) \quad \text{(A6)}$$

Defining statistical operator $\langle . \rangle$, for average over a large number $\mathcal{N}_p$ of realisation $\mathcal{H}_p$ for a given realisation $\mathcal{H}_f$, as

$$<g\left|\mathcal{H}_f\right.>=\frac{1}{\breve{n}_p(\mathbf{x},\tau,\mathcal{H}_f)}\int g\ \breve{f}_p^{(1)}(\mathbf{x},\mathbf{c}_p,\xi_p,\tau,\mathcal{H}_f)d\mathbf{c}_p d\xi_p \quad \text{(A7)}$$

one can write high order moments characterizing Quasi-Brownian velocity and temperature, that are, in order, the uncorrelated kinetic stress tensor , the uncorrelated kinetic energy, the third moment correlation

$$\delta R_{p,ij}(\mathbf{x},\tau,\mathcal{H}_f)=\left\langle\delta v_{p,i}\delta v_{p,j}\left|\mathbf{x}_p(\tau)=\mathbf{x};\mathcal{H}_f\right.\right\rangle \quad \text{(A8)}$$

$$\delta\theta_p(\mathbf{x},\tau,\mathcal{H}_f)=\frac{1}{2}\left\langle\delta v_{p,i}\delta v_{p,i}\left|\mathbf{x}_p(\tau)=\mathbf{x};\mathcal{H}_f\right.\right\rangle \quad \text{(A9)}$$

$$\delta Q_{p,ijk}(\mathbf{x},\tau,\mathcal{H}_f)=\left\langle\delta v_{p,i}\delta v_{p,j}\delta v_{p,k}\left|\mathbf{x}_p(\tau)=\mathbf{x};\mathcal{H}_f\right.\right\rangle \quad \text{(A10)}$$

and the uncorrelated heat flux and the uncorrelated temperature variance

$$\delta\Theta_{p,i}(\mathbf{x},\tau,\mathcal{H}_f)=\left\langle\delta v_{p,i}\delta t_p\left|\mathbf{x}_p(\tau)=\mathbf{x};\mathcal{H}_f\right.\right\rangle \quad \text{(A11)}$$

$$\delta\theta_\theta(\mathbf{x},\tau,\mathcal{H}_f)=\left\langle\delta t_p\delta t_p\left|\mathbf{x}_p(\tau)=\mathbf{x};\mathcal{H}_f\right.\right\rangle \quad \text{(A12)}$$

Copyright © 2008 by ASME

Downloaded From: https://proceedings.asmedigitalcollection.asme.org on 06/30/2019 Terms of Use: http://www.asme.org/about-asme/terms-of-use